

## 11. MELT-FLUID EVOLUTION IN GABBROIC ROCKS FROM HESS DEEP<sup>1</sup>

Deborah S. Kelley<sup>2</sup> and John Malpas<sup>3</sup>

### ABSTRACT

Mineralogical and fluid inclusion analyses of gabbroic rocks recovered from Site 894 on the intrarift ridge at Hess Deep indicate that the gabbroic sequence is a product of a complex history involving multiple magmatic and hydrothermal events. Pegmatitic patches throughout the core that contain high concentrations of apatite, zircon, oxide minerals, and coarse-grained amphibole are believed to have crystallized under relatively high  $fO_2$  from a hydrous magma. The patches of micropegmatite represent the most evolved compositions sampled at Site 894 and may reflect reequilibration with evolved, volatile-rich fluids that percolated through the gabbroic sequence late in the magmatic history. Analyses of fluid inclusions entrapped within these zones, indicate that 30–40 wt% NaCl  $\pm$  Fe  $\pm$  CO<sub>2</sub>-rich brines formed either under immiscible conditions in association with the evolved patches, or were exsolved in the absence of a vapor phase directly from the compositionally evolved melts. Migration of the high-salinity fluids may have resulted in the crystallization of apatites that contain up to ~6 wt% chlorine.

The transition from magmatic to hydrothermal seawater-dominated conditions in the plutonic sequence is marked by penetration of fluids that exhibit equivalent fluid salinities that range from ~0.1% to 200% of seawater values (3.2 wt% NaCl) and exhibit uncorrected homogenization temperatures that cluster at ~250°C. The extremely low-salinities were most likely formed during supercritical phase separation of seawater at temperatures >407°C. Their preservation requires that the vapor phase remained isolated from the associated brine and that subsequent mixing with seawater did not occur. The compositions of the plutonic-hosted fluids are similar to those of fluids exiting hydrothermal vents, indicating that the fracture networks may represent the feeder systems for sustained hydrothermal flow. Migration of these fluids along microfracture and vein networks resulted in the heterogeneous replacement of the gabbroic rocks by greenschist facies mineral assemblages. This alteration is most intense adjacent to vein networks and in cataclastically deformed zones, in which brittle failure facilitated enhanced fluid flow. Sealing of the microfracture and fracture networks with zeolite facies mineral assemblages marks the cessation of fluid circulation in the plutonic sequence. The plutonic sequence may have undergone as much as 2 km of uplift attendant with crustal thinning and propagation of the Cocos-Nazca spreading center.

### INTRODUCTION

One of the least understood relationships in the construction of the oceanic lithosphere is the interaction between magmatic and hydrothermal processes. Most workers, either dealing with in situ oceanic crust or with ophiolites, have tended to focus their efforts on each or both sets of processes independently, with little emphasis on the manner in which they interplay and overlap. The relationship between these processes is likely to be different at spreading centers that evolve at different spreading rates; particularly because it appears that the depth and extent of processes related to amagmatic spreading might be greater in slower spreading environments as the magma supply rate most likely has an effect on the depth of the brittle/ductile boundary (Toomey et al., 1985; Riedesel et al., 1982; Sinton and Detrick, 1992). Enhanced hydrothermal flow, facilitated by brittle fractures, would thus be pervasive to greater depth close to a slow-spreading ridge compared to a fast-spreading system. Observations made at the Southwest Indian Ridge (SWIR) during Ocean Drilling Program (ODP) Leg 118 certainly support the fact that magmatism, tectonism, and hydrothermal activity are strongly related at slow-spreading (8–12 mm/yr) ridges (Dick et al., 1991). The coupled evolution of magma-hydrothermal systems in fast-spreading ridge environments has not been well characterized, predominantly owing to the inherent difficulty in sampling deep crustal levels. If seismic data from fast-spreading ridges are interpreted to indicate that the brittle-

ductile transition occurs at the roof of a sub-rift magma chamber (Huang and Solomon, 1988), or that ductile deformation is indeed absent, then seawater is unlikely to pervasively percolate into the early formed oceanic crust and thus, high-temperature metamorphism might not be nearly so significant in fast-spreading systems. For such reasons it is important to obtain samples of the plutonic section (Layer 3) of the oceanic crust by deep drilling in areas that have experienced different spreading rates, for example, slow-spreading on the Southwest Indian Ridge (Leg 118, Hole 735B) or near the southern intersection of the Kane Fracture Zone and the Mid-Atlantic Ridge (MARK; Leg 153, Sites 921–924), and fast-spreading on the East Pacific Rise (Leg 147, Sites 894 and 895).

In late 1992 to early 1993, ODP drilled Sites 894 and 895 at the Hess Deep to investigate the evolution of magma supply to the sub-rift magma chamber system of the fast-spreading East Pacific Rise (EPR) and the effects of contiguous high-temperature deformation and hydrothermal alteration. Hess Deep is the deepest portion of an oceanic rift valley that is propagating westward into the eastern flank of the EPR ahead of the Cocos-Nazca spreading center (Fig. 1). At a distance of some 70 km east of the EPR axis, uplift of lower crustal and mantle rocks attendant with propagation of the Cocos-Nazca spreading center has built a median ridge in the rift valley with a relief of as much as 2700 m. A complete but structurally dissected crustal section of the EPR including peridotite, gabbro, diabase, and basalt has been sampled during a submersible cruise in this area (Francheteau et al., 1990) and by ODP drilling on Leg 147 at Sites 894 and 895. The distribution of these rock types indicates that there is severe structural dismemberment of the crustal and upper mantle stratigraphy. There appears to be little lateral continuity and in places there is a clear reversal of normal lithospheric stratigraphy where harzburgites of the upper mantle sequence overlie cumulate gabbros of Layer 3. In addition, the western portion of the ridge is dominated

<sup>1</sup>Mével, C., Gillis, K.M., Allan, J.F., and Meyer, P.S. (Eds.), 1996. *Proc. ODP, Sci. Results, 147*: College Station, TX (Ocean Drilling Program).

<sup>2</sup>School of Oceanography, University of Washington, Seattle, WA, 98195, U.S.A. kelley@ocean.washington.edu

<sup>3</sup>Department of Earth Sciences, Memorial University, St. John's, Newfoundland, A1B 3X5, Canada. odp@kean.ucs.mun.ca

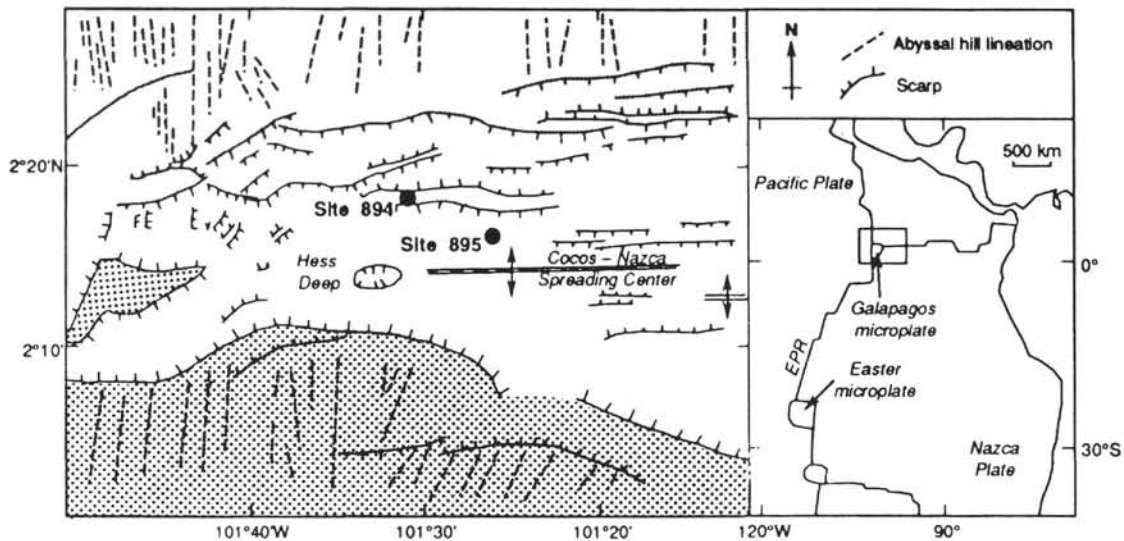


Figure 1. Location of Hess Deep at the western end of the propagating Cocos-Nazca spreading axis.

by gabbros and gabbro-norites, and the eastern end by rocks from higher in the stratigraphic sequence that include diabase and basalt (Francheteau et al., 1990; Gillis, Mével, Allan, et al., 1993).

At Site 894, located at the western end of the intrarift ridge, a series of offset holes was cored during Leg 147, from which a sequence of high-level gabbroic rocks was recovered. At Site 895, some 9 km southeast of Site 894, the sequence of ultramafic and mafic rocks recovered included dunites and harzburgites with associated troctolites, gabbros, and basalts. Rocks recovered from Site 894 were considered by the shipboard scientific party to have developed in the roof zone of an axial magma chamber, and those from Site 895 from the transition zone between Layer 3 of the oceanic crust and the upper mantle (Gillis, Mével, Allan, et al., 1993). The gabbroic and mantle rocks represent the first in situ plutonic rocks recovered from a fast-spreading environment and allow comparison of the well-studied magmatic and hydrothermal process found at slow-spreading oceanic systems such as the SWIR and MARK areas. In this study, mineralogical, geochemical, and fluid inclusion analyses on gabbroic rocks recovered from Site 894 are used to investigate the relationship between magmatic, deformational, and hydrothermal processes in the upper plutonic section of crust formed in a fast-spreading system.

#### Site 894

At Site 894 a series of seven holes was drilled near the crest of the intrarift ridge (Holes 894A–894G). Together, Holes 894F and 894G represent significant penetration into the upper parts of oceanic crustal Layer 3. Drilling at Hole 894F penetrated 25.7 m below seafloor (mbsf) and recovered 1.8 m of deformed and cataclased gabbros and olivine gabbros cut by aphyric basaltic dikes. At Hole 894G, drilled 10 m west of Hole 894F, penetration was 154.5 mbsf and 45.78 m of core was recovered. In this hole, the upper 18.6 m was not cored because an equivalent section was recovered in Hole 894F.

The igneous lithologies recovered in Holes 894F and 894G include gabbro-norite, gabbro, olivine gabbro, olivine gabbro-norite, and basalt. On a hand-sample scale, the textures displayed by these rocks are equivalent to those of the varitextured gabbros found in ophiolites generally toward the upper boundary of the plutonic sequence and immediately below the sheeted dikes (Pedersen and Malpas, 1984; Pedersen, 1986). Indeed, this is the most likely location of Site 894, albeit in the highly structurally dissected crustal stratigraphy exhibited at Hess Deep. Although recognized widely in ophiolite sequences, these rocks have only rarely been worked on in any detail (Pedersen,

1986; Kelley et al., 1992), and have never been collected in significant quantities from the ocean basins. In ophiolite suites, varitextured gabbros are in many places associated with oxide-rich diorites and plagiogranitic rocks. The similarity of the varitextured gabbroic rocks from Site 894 to those from ophiolites suggests that they might be ideal for the investigation of magma-fluid evolution in the upper parts of a sub-rift magma chamber.

#### PETROGRAPHY OF GABBROIC ROCKS FROM HOLE 894G

The characteristic feature of the gabbroic rocks from Hole 894G is their abrupt change in grain size, texture, and modal mineralogy on a hand-sample scale. This variety of textures is not regular and grain sizes vary from micropegmatitic to aphanitic over short distances. Hence the term "varitextured." Gabbro-norites represent the most voluminous rock type recovered at Site 894 (77.4%) and they grade in a reduction in their modal orthopyroxene content to gabbros. Many of the gabbroic rocks exhibit poikilitic textures with anhedral oikocrysts of orthopyroxene and minor clinopyroxene that contain chadacrysts of resorbed olivine with which there exists a reaction relationship. Elsewhere, a variety of textural types between intergranular and hypidiomorphic granular has been recognized. Some gabbro-norites are clearly more plagioclase-rich than others, and there is sporadic enrichment of Fe-Ti oxide minerals (e.g., Section 147-894G-13R-1). These latter rocks and other gabbro-norites that are among the more coarse-grained or micropegmatitic samples are of particular importance here in that they are characterized by concentrations of zircon and apatite (Figs. 2, 3). Both of these minerals are associated with primary phases that include dark green to brown-amber amphibole. Clusters of euhedral, rhombic, and acicular zircons are in places intergrown with the associated primary oxide minerals. Smaller concentrations of acicular or stubby apatite are typically partly enclosed by the amphibole, which indicates co-crystallization. These micropegmatitic patches and pods are typically the most fluid inclusion-rich zones in the core, and are generally the only areas in which halite-bearing fluids are entrapped (see "Fluid Inclusion" discussion). Where it has been possible to isolate some of the micropegmatitic material for whole-rock analysis, the chemistry indicates that these patches of micropegmatite represent the most evolved compositions sampled at Site 894. These relationships are illustrated by Sample 153-894G-9R-3, 80–83 cm (Piece 5D) (Table 1), which has

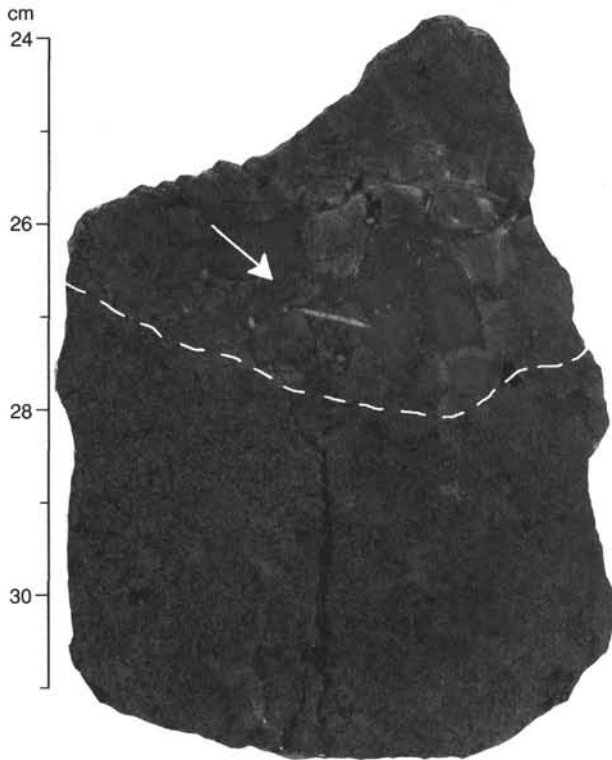


Figure 2. Micropegmatitic gabbronorite with centimeter-long apatite needles (arrow) (Sample 147-894G-17R-1, 24–31 cm (Piece 6)).

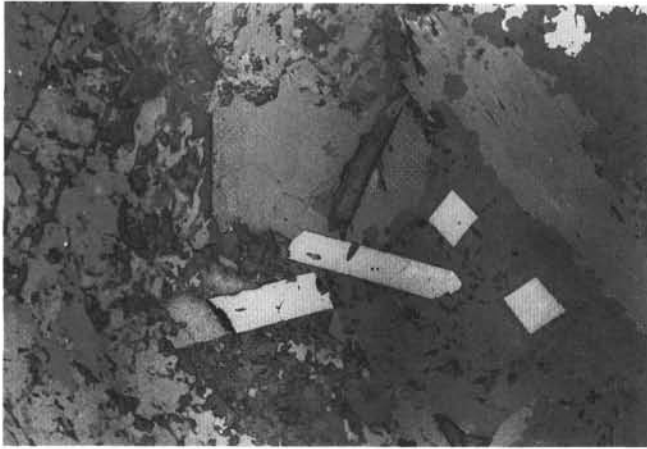


Figure 3. Reflected light photomicrograph of euhedral zircon (white) in micropegmatitic patch in gabbronorite (Sample 147-894G-9R-3, 48–50 cm [Piece 4]). Field of view is 1.5 mm.

2.23 wt%  $\text{TiO}_2$ , 1.01 wt%  $\text{P}_2\text{O}_5$ , and high V, Y, Zr, and Nb with relatively depleted Cr. Based on the textural relationships, mineralogy, and chemistry, we thus believe this assemblage to be late magmatic or deuteric in origin and to have crystallized from an evolved fluid-rich silicate magma.

Another texture of particular interest in the gabbroic rocks and recognizable only in thin section occurs as 1–3-mm patches in some of the medium-grained poikilitic gabbronorites. These small areas exhibit ill-defined boundaries that are cored with clinopyroxene minerals that exhibit ophitic to subophitic textures, and that are replaced in part by amphibole. Based on the textural relationships, these patches are believed to be altered and partially resorbed diabase inclusions.

Table 1. Representative whole-rock compositions from micropegmatitic patches.

Oxides	wt%	Trace elements	ppm	REE	ppm
$\text{SiO}_2$	49.78	V	356	La	15.86
$\text{TiO}_2$	2.23	Cr	172	Ce	45.78
$\text{Al}_2\text{O}_3$	9.88	Co	53	Pr	7.30
$\text{Fe}^{\text{total}}$	15.89	Ni	83	Nd	35.41
MnO	0.2	Cu	8	Sm	11.06
MgO	8.5	Zn	52	Eu	2.09
CaO	10.08	Rb	0	Gd	14.81
$\text{Na}_2\text{O}$	2.49	Sr	78	Tb	2.35
$\text{K}_2\text{O}$	0.01	Y	106	Dy	15.00
$\text{P}_2\text{O}_5$	1.01	Zr	714	Ho	3.19
LOI	0.92	Nb	12	Er	9.04
Sum	100.99	Ba	3	Tm	1.23
S	0.063	Pb	0	Yb	7.54
		Th	5	Lu	1.23
		U	1		
		Mo	0		

Notes: Sample 147-894G-9R-3, 80–83 cm (Piece 5D); depth = 76.79 mbsf.

Such a feature would not be out of place at the upper margin of a magma chamber in contact with overlying sheeted dikes.

## MINERALOGY AND CRYSTAL CHEMISTRY

Analysis of major silicate phases was conducted on a Cameca SX-50 electron microprobe in energy dispersive mode for major elements and wavelength dispersive mode for minor elements. Multiple points were analyzed for each phase both in individual crystals and throughout each thin section.

### Plagioclase

Plagioclase forms approximately 50% to 55% of the mode throughout most of the gabbroic rocks recovered from Hole 894G. Although most of the plagioclase grains are subhedral, lath-shaped crystals, more euhedral crystals are found in the micropegmatitic rocks, especially where there is enrichment of plagioclase to as much as 75% of the mode. In these micropegmatitic patches, the plagioclase grain size varies from 0.01 to 8 mm with two population peaks at approximate averages of 0.5 and 2 mm, respectively. Optical zoning is common and can be normal, reverse, oscillatory, or patchy in nature (Fig. 4) (Pedersen et al., this volume). Throughout Hole 894G, the range of An contents is from  $\text{An}_{87}$  to  $\text{An}_{44}$ , but whereas there are variations between plagioclase grains in single thin sections (up to An 25%), there is no distinct trend in the overall average An content of the plagioclase in rocks from the top to the bottom of the hole. One notable correlation, however, is that plagioclase phases from the micropegmatitic patches have average An contents distinctly lower than the norm (Fig. 5A). This relationship corresponds with the more evolved nature of these patches as a whole.

### Ferromagnesian Minerals

#### Orthopyroxene

In the Site 894 gabbronorites, orthopyroxene forms up to 20% of the mode as either large anhedral oikocrysts or as euhedral to subhedral, granular primocrysts. Both forms are strongly pleochroic from  $x = \text{pale pink}$ ,  $y = \text{pale yellow}$ , to  $z = \text{pale green}$ , and they appear unzoned. In some thin sections, the crystals are embayed and almost everywhere exhibit exsolution lamellae of clinopyroxene. It is apparent that the Mg content of the orthopyroxenes is relatively consistent with depth (average  $\text{En}_{68}$ ) except for values in granular primocrysts as low as  $\text{En}_{61}$  at 76.79 mbsf and  $\text{En}_{63.5}$  at 100.23 mbsf (Fig. 5B),





Figure 4. Optical zonation in plagioclase (Sample 147-894G-12R-2, 91–96 cm [Piece 9A]). Field of view is 3.5 mm

which correspond to low bulk-rock Mg numbers and low Mg numbers in coexisting pyroxene phases (Pedersen et al., this volume). These more Mg-poor (Fs-rich) hypersthene primocrysts are found in the micropegmatitic gabbronorites that contain impressive concentrations of zircon, apatite, and oxide minerals; have the most evolved plagioclase compositions; and in at least one case, bulk rock Zr as high as 714 ppm (Table 1; Sample 153-894G-9R-3, 80–83 cm [Piece 5D]). This supports the conclusion that the micropegmatitic pods crystallized from (or reequilibrated with) relatively evolved interstitial liquid that had accumulated in these patches.

Both Cr and Ti in the orthopyroxenes occur in amounts common in oceanic gabbroic rocks from other localities. Although in general neither Cr or Ti show a clear fractionation trend when plotted against Mg (Pedersen et al., this volume), the Cr content of the orthopyroxenes from the micropegmatitic patches is lower than in orthopyroxenes from elsewhere in the section. No such clear relationship exists for Ti (Fig. 6).

### Clinopyroxene

Clinopyroxene occurs throughout the sequence in Hole 894G with an average modal abundance of 32%. It, like orthopyroxene, occurs as oikocrysts and as anhedral equigranular crystals together with plagioclase. Clinopyroxene is weakly zoned with core to rim values of  $En_{73}$  to  $En_{64}$  (Fig. 6). More evolved clinopyroxene core compositions ( $En_{59}$ ) occur in the micropegmatitic gabbronorite at 106.7 mbsf (Core 147-894G-13R), corresponding to a low Mg number in the bulk rock. There is little decrease in En values of coexisting orthopyroxene minerals, however (Pedersen et al., this volume). The occurrence of numerous thin exsolution lamellae of orthopyroxene and incipient alteration along cleavage planes to amphibole, even in the freshest samples, makes analyses difficult.

### Late Magmatic Phases

Zircon and apatite minerals are particularly abundant in the micropegmatitic patches where they locally form a striking characteristic of the core on a hand-sample scale (Figs. 2, 3). Zircon forms euhedral prismatic crystals with habits ranging from rhombic to acicular (Fig. 3). Clusters of zircon are intergrown with adjacent opaque oxide minerals. Apatite generally occurs as fine-grained stubby crystals, although coarser grained acicular needles (up to 1 cm long) have been identified (Fig. 2). Compared to surrounding mineral phases, the apatites are anomalously rich in both primary and secondary fluid inclusions (see fluid inclusion discussion). The apatites, which show

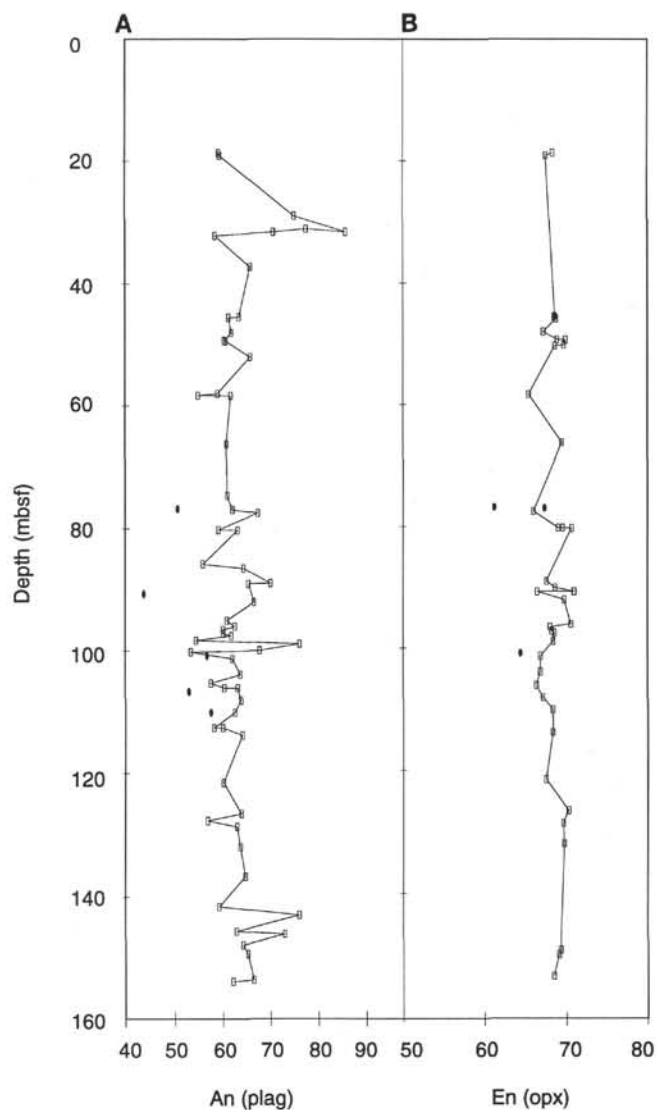


Figure 5. **A.** Average An composition in plagioclase vs. depth in Hole 894G. Values in individual samples vary by  $\pm An_{1.7\%}$ . **B.** Average En compositions of orthopyroxenes vs. depth in Hole 894G. Values in individual samples vary by  $(\pm En_{0.8\%})$ . Solid symbols = micropegmatitic patches in gabbronorite. Open symbols = other gabbroic rocks.

classic normalized rare earth element (REE) distributions, contain 0.4 to 1.0 wt% fluorine, and up to 5.8 wt% chlorine (K. Gillis, unpubl. data). The chlorine values are some of the highest concentrations reported for mid-ocean ridge environments. Amphibole occurs as blue-green, olive green, and zoned bladed crystals with brown cores and amber rims and as finer-grained, fibrous patches in the micropegmatitic pods. Most of the amphibole compositions in the Hole 894G rocks lie in a compositional range between actinolite and magnesiohornblende (Gillis, this volume). CaO and FeO increase sympathetically, and although  $Al^{IV}$  content increases with Site A occupancy and Ti content, there is no consistent variation in composition with depth, and mixtures of low-Al and high-Al amphiboles are not uncommon. According to Gillis (this volume), anomalous enrichment of REE for some of the amphiboles associated with the micropegmatitic patches indicates that they are most likely primary in origin, having crystallized from an evolved melt enriched in light REE.

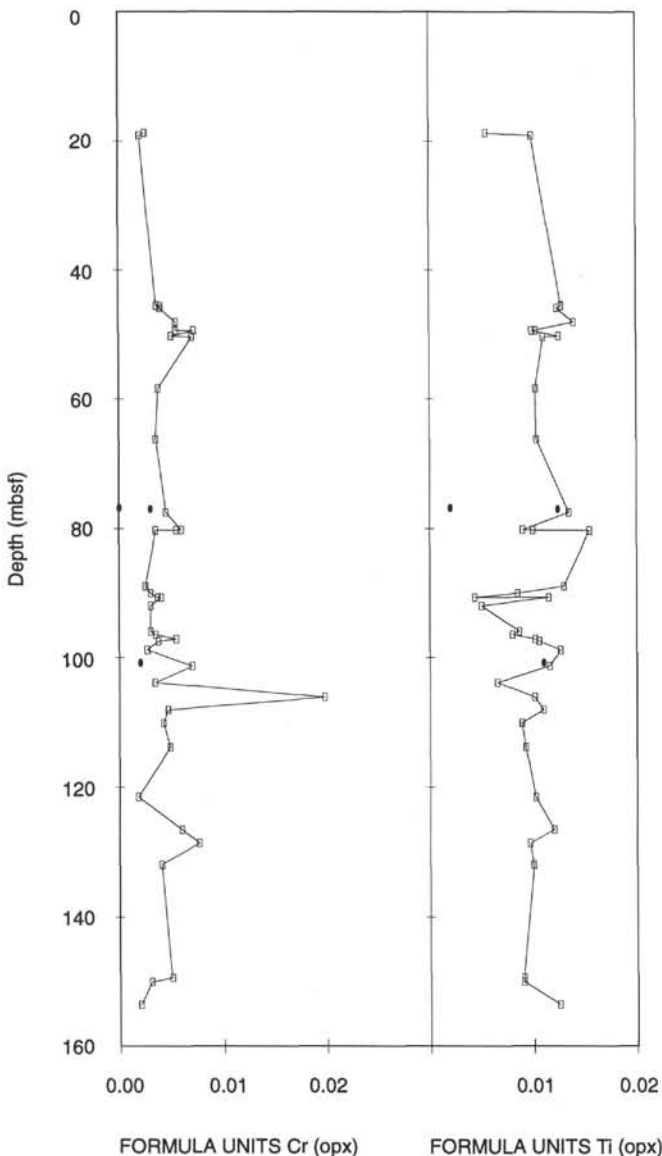


Figure 6. Average Cr and Ti contents of orthopyroxenes vs. depth in Hole 894G. The maximum and minimum values for both Cr and Ti vary by  $\pm 0.001$ . Solid symbols = micropegmatitic patches in gabbro. Open symbols = other gabbroic rocks.

## METAMORPHISM

The 45-m section of variably altered and deformed gabbro, olivine gabbro, and oxide gabbro recovered from Hole 894G records a complex history of interaction between magmatic, deformational, and hydrothermal processes. Interaction with hydrothermal fluids resulted in static metamorphism under amphibolite to zeolite facies conditions, with at least 80% of the gabbros drilled affected by 20%–50% background replacement by secondary minerals. Locally, in intensely deformed zones associated with cataclastic deformation and in net-veined zones, alteration is pervasive. Background static metamorphism of the gabbroic rocks is heterogeneous and variable both on a centimeter and several meter scale, reflecting variation in fracturing and attendant hydration. The earliest alteration phases typically occur along grain boundaries and fine veinlets and generally consist of fine-grained amphibole. The irregular microscopic network of actinolitic veins that are common rimming grain boundaries and that form an anastomosing network, cutting grains is ubiquitous

in the gabbroic rocks. This fracture system most likely facilitated fluid flow into the gabbroic sequence, resulting in the background alteration. Macroscopic veins are most commonly composed of actinolite and chlorite, with rare, later veins filled by variable amounts of chlorite, smectite, prehnite, epidote, and actinolite (see Manning and MacLeod, this volume).

## Olivine

Olivine alteration is highly variable and involves complex and heterogeneous coronitic replacement. Though alteration is commonly pervasive, some samples contain up to 90% relict olivine. Irregular to concentric zonation replacement of olivine by secondary phases includes variable amounts of talc, magnetite, mixed-layer chlorite smectite, Ca-Al amphibole, and cummingtonite. Where olivine grains are in contact with plagioclase, highly zoned, rimming bands of pale green chlorite with anomalous blue to olive green birefringence are common. Olivine grains are rarely cut by liquid to vapor-rich fluid inclusion arrays.

## Clinopyroxene

Alteration of clinopyroxene dominates the alteration intensity in the gabbroic rocks. Clinopyroxene grains exhibit variable degrees of alteration with the most intensely altered grains commonly occurring in micropegmatitic patches. Magnesio-hornblende as fine-grained inclusions in clinopyroxene is common. With increasing alteration fibrous rims of actinolitic hornblende and associated fine-grained oxide minerals are common. The secondary amphibole is the most common hydrothermal mineral in the gabbroic rocks, replacing olivine, clinopyroxene, and plagioclase. Felted actinolitic mats after clinopyroxene form distinctive amoeboid-shaped pods, and are most common in alteration halos associated with veins. In localized patches and in micropegmatitic zones, hydrothermal clinopyroxene is common, where it forms as turbid to clear irregular patches on primary clinopyroxene and as monomineralic grains. The pyroxene is distinguished petrographically from strictly magmatic pyroxenes by its pale green color, an absence of exsolution lamellae, and ubiquitous primary fluid inclusions. Based on pyroxene geothermometry, compositions of the hydrothermal clinopyroxenes indicate that they formed at minimum temperatures of 650°C–800°C (Gillis, this volume; Manning and MacLeod, this volume). The fluid inclusion-rich clinopyroxenes are similar to those in gabbroic rocks recovered from MARK (Kelley and Delaney, 1987; Gillis et al., 1993; Kelley et al., 1993) and from ODP Hole 735B on the SWIR (Stakes et al., 1991; Kelley et al., 1993).

## Orthopyroxene

Orthopyroxene alteration ranges from moderate to pervasive, with finer grains commonly more pervasively altered. Similar to clinopyroxene, secondary replacement of orthopyroxene is heterogeneous on a thin-section to hand-sample scale. Cummingtonite and fine-grained oxide minerals typically fill microfractures cutting orthopyroxene grains, form narrow rims around the grains, and occur as isolated fibrous patches within the grains. In zones where alteration minerals are well developed, pale green to yellow, coarse-grained amphibole commonly rims orthopyroxene. Replacement by talc and pargasitic hornblende is rare (Gillis, this volume).

## Plagioclase

Alteration of plagioclase ranges from <10% to 100% and predominantly involves the formation of secondary plagioclase, with lesser amounts of actinolite, chlorite, epidote, prehnite and zeolite, and clay minerals. Alteration is most intense adjacent to crosscutting veins and vein networks and within cataclastic deformation zones. Locally, in extensively altered patches and adjacent to veins, the plagioclase

is turbid and dusty in appearance owing to replacement by secondary plagioclase, clay, and zeolite minerals. In these zones, the secondary plagioclase is characterized by containing abundant anhedral to euhedral, liquid-dominated fluid inclusions that range in size from <5 to 40  $\mu\text{m}$ . The inclusions are especially well developed in micropegmatitic patches and may contain halite-daughter minerals. Fine-grained, fibrous sprays of actinolite intergrown with chlorite commonly rim grain boundaries and fill microfractures that crosscut the plagioclase grains. Locally, the plagioclase is rimmed and cut by clear, discontinuous veinlets of potassium feldspar (Gillis, this volume). In the micropegmatitic zones, epidote forms fine-grained, pale green granular to bladed inclusions within plagioclase.

## FLUID INCLUSIONS

Fluid inclusions entrapped in successive generations of magmatic and alteration minerals provide the only direct information on fluids circulating in the crust and, therefore, are a unique window into the evolution of magmatic volatiles and circulation of seawater at depth. They provide physicochemical information for fluids which has not been predicted from alteration studies (i.e., the discovery of immiscible brines, vapors, and methane-rich fluids [Kelley et al., 1993; Kelley and McDuff, 1993]), and have been used to constrain the uplift histories of outcropping submarine plutonic rocks (Kelley and Delaney, 1987; Vanko, 1988; Kelley et al., 1993).

Multiple populations of fluid inclusions in the variably altered and deformed gabbroic rocks recovered from Hess Deep indicate that fluid circulation at Site 894 involved fluids of widely varying composition and temperature, and was probably initiated at late magmatic conditions. Fluid inclusions are abundant in the gabbroic matrix minerals, where they occur along healed microfractures, and less common as primary inclusions trapped during the growth of primary and secondary minerals. They are strikingly abundant in apatite and plagioclase within the pegmatitic pods, and provide important information on the fluids involved in the formation and alteration of these patches. In vein minerals, the rare primary and secondary inclusions probably reflect the inherent difficulty of minerals such as actinolite, chlorite, and prehnite to trap fluid inclusions. In the following discussion, compositional and thermal analyses of the entrapped fluids are presented.

### Methods

Microthermometric analyses of fluid inclusions were conducted on a Fluid Inc. adapted U.S. Geological Survey (USGS) gas-flow heating and freezing stage according to the procedures outlined by Roedder (1984). Replicate homogenization and freezing measurements were carried out on individual inclusions in order to obtain corresponding homogenization temperatures and fluid salinities. Homogenization and dissolution temperatures were measured during progressive heating of the sample in order to avoid decrepitation and potential alteration of phase-change temperatures resulting from stretching and leaking. To obtain a representative sampling of inclusion populations, each reported analysis typically represents measurements of a subpopulation of four to five individual inclusions along an array of inclusions, or of a cluster of primary inclusions, in which all inclusions displayed consistent phase ratios and behaved similarly. Inclusions along individual microfractures or primary clusters were homogenized within 5°C–10°C of adjacent inclusions. The stage was calibrated by presetting the instrument to yield the temperatures of phase transitions of synthetic fluid inclusions at –56.6°C, 0.0°C, and +374°C. All analyses were reproducible to within 0.1°C. Unsaturated and saturated salinities were obtained using the equations of Bodnar (1993) and Sterner et al. (1988) and are reported in terms of NaCl equivalent. Homogenization temperatures have not been corrected for pressure effects (see “Temperatures of Fluid Entrapment” section).

## FLUID INCLUSION TYPES AND RESULTS

Fluid inclusion types were described and classified petrographically at room temperature previous to microthermometric analyses. Primary inclusions in apatite and plagioclase occur as tubular euhedral inclusions oriented parallel to crystal faces; however, in some grains, inclusions are so abundant that it is impossible to unambiguously determine inclusion origin. In hydrothermal clinopyroxene, primary inclusions that form parallel to crystal faces are ubiquitous. They are typically vapor-dominated, though they may also exhibit variable vapor-to-liquid ratios. Secondary fluid inclusions along healed microfractures are especially common in plagioclase, although they also occur in apatite, epidote, and amphibole. Abbreviations for inclusion homogenization behavior are as follows [Th L+V (L)] indicates the temperature of homogenization for liquid + vapor inclusions that homogenize to the liquid phase (i.e., by disappearance of the vapor bubble); [Tm < Th L+V (L)] indicates the temperature of homogenization for halite-bearing inclusions in which halite dissolution occurs prior to vapor bubble disappearance and that the inclusions homogenize into the liquid phase; and [Tm > Th L+V (L)] indicates the temperature of homogenization for halite-bearing inclusions in which halite dissolution occurs subsequent to vapor bubble disappearance. Based on petrographic analyses at room temperature, the inclusions were classified into three main types; results of microthermometric analyses of these inclusions are presented in Table 2.

### Type 1: Liquid-dominated, Low-salinity Inclusions

Gabbro-hosted, liquid-dominated, low-salinity fluid inclusions are pervasive in plagioclase and less common in apatite, epidote, and amphibole (Table 2). Only plagioclase- and apatite-hosted inclusions were measured in this study. In plagioclase, these low-temperature inclusions commonly exhibit negative to irregular crystal habits and form anastomosing arrays along healed microfractures, which indicates that the inclusions are secondary (Fig. 7A). More rarely, the inclusions form concentrated zones of irregularly to euhedral-shaped inclusions that occur in turbid patches of secondary plagioclase and in clear zones of secondary plagioclase that rim plagioclase. The plagioclase-hosted inclusions homogenize to the liquid phase [Th L+V (L)] at temperatures of 207°C–323°C and contain equivalent salinities of 0.1–13.4 wt% NaCl (Table 2; Figs. 8–10). Apatite-hosted inclusions homogenize to the liquid phase at temperatures of 216°C–372°C and contain equivalent fluid salinities of 0.2–19.3 wt% NaCl (Table 2; Fig. 8). In Sample 147-894G-13R-1, 132–136 cm (Piece 14), the inclusions that contain fluids with ~15–20 wt% NaCl equivalent salinities are optically difficult for determining homogenization temperatures; therefore, the 325°C–370°C temperatures are minimum homogenization temperatures for these inclusions (arrows on Figs. 8 and 9).

### Type 2: Vapor-dominated, Low-salinity Inclusions

Vapor-dominated, low-salinity inclusions are common in hydrothermal clinopyroxene as primary inclusions, and are less common as primary(?) and secondary inclusions in epidote. They are rare in apatite. Homogenization temperatures and freezing measurements were not collected on these inclusions.

### Type 3: Daughter Mineral-bearing Inclusions

Halite-bearing inclusions in plutonic samples from Hess Deep (Table 2) occur in apatite and plagioclase as primary(?) and secondary inclusions (Fig. 7B). In many grains, inclusions are so abundant that an unequivocal origin of the inclusions cannot be determined. Halite daughter minerals that contain an opaque cubic daughter mineral, tentatively identified as pyrite, are rare. The brine-rich inclu-



**Table 2. Summary of fluid inclusion analyses in gabbroic rocks recovered from Hole 894G, Hess Deep.**

Core, section, interval (cm)	Rock type	Mineral host	Type	Number	Th (°C)			NaCl (wt%)			Comments
					Range	Average	s.d.	Range	Average	s.d.	
147-894G- 4R-2, 42–46 (Piece 8)	Gabbro: p egmatitic patch	Plagioclase	1	17	Metagabbro 228–268 253 11.7			1.3–13.4	4.0	3.0	Th L + V (L), secondary
6R-1, 138–142 (Piece 12)	Gabbro: p egmatitic patch	Plagioclase	1	19	207–250	228	10.8	1.8–6.7	3.2	1.9	Th L + V (L), secondary
9R-2, 58–63 (Piece 3)	Gabbro: p egmatitic patch	Plagioclase	1	33	209–323	281.4	26.8	0.1–4.2	1.2	1.2	Th L + V (L), primary(?) and secondary, hosted in clear rims of plagioclase, rare brines
9R-3, 51–55 (Piece 4)	Gabbro: p egmatitic patch	Plagioclase	1	27	231–289	257	15.4	0.8–5.4	2.5	0.9	Th L + V (L), secondary
		Plagioclase	3	11	248–308	273	30.3	34–39	36	2.0	Tm > Th L + V (L), secondary*
		Apatite	3	14	181–347	241	61.3	31–33	32	0.5	Tm < Th L + V (L), primary(?) and secondary(?)**
13R-1, 132–136 (Piece 14)	Gabbro	Apatite	1	20	216–372	250.7	44	0.2–19.3	2.9	6.4	Th L + V (L), secondary, two populations (minimum Th for high-t inclusions)
20R-1, 1–4 (Piece 1)	Gabbro: p egmatitic patch	Plagioclase	1	24	210–262	236	13.3	2.1–11.2	3.5	2.0	Th L + V (L), secondary
		Apatite	3	8	264–305	283	16	29–30	30	0.3	Tm < Th L + V (L), primary and secondary**

Notes: Th = homogenization temperature; average of all measurements; s.d. = standard deviation; Th L + V (L) = liquid + vapor inclusions homogenizing in the liquid phase; Tm = halite dissolution; Type 1 = liquid-dominated secondary; Type 3 = liquid-dominated, halite-bearing. \* = homogenized by halite dissolution, therefore Th = Tm. \*\* = some inclusions exhibit an increase in bubble size on cooling, and one inclusion exhibited a clathrate melting temperature of +9.9°C, which indicates that the inclusions most likely contain CO<sub>2</sub> + H<sub>2</sub>O + NaCl.

sions, which are liquid-dominated to vapor-rich, exhibit two types of homogenization behavior on heating. Inclusions that lie in the field just to the right of the inclusions labeled Tm > Th L+V (L) in Figure 8 and the liquid + vapor + halite curve in Figure 9 homogenize by vapor bubble disappearance at temperatures [Tm < Th L+V (L)] of 193°C–346°C and exhibit halite dissolution temperatures of 144°C–218°C (Fig. 11). Halite dissolution temperatures indicate that the inclusions contain fluid salinities of 29–32 wt% NaCl equivalent. Uncommonly, liquid-dominated inclusions exhibit indirect evidence for the presence of dissolved gas and of clathrate formation on cooling (Table 2). The observation of expansion of the vapor phase on cooling in some vapor-rich, halite-bearing inclusions (Samples 147-894G-9R-3, 51–55 cm [Piece 4] and 894G-9R-3, 80–83 cm [Piece 5D]) and of clathrate melting temperatures of +9.9°C observed in one sample (Sample 147-894G-20R-1, 1–4 cm [Piece 1]) indicates that these inclusions most likely contain CO<sub>2</sub>, though melting events at –56.6°C were not observed. Future crushing experiments and micro-Raman spectroscopic analyses are needed to confirm the presence of volatile phases and to determine the composition of the entrapped volatile species in these inclusions. Halite-bearing inclusions that exhibit temperature-compositional relationships that form the gently sloped curve shown in Figures 8 and 9, and that fall in the field to the left of the dashed line in Figure 11, homogenize by halite dissolution [Tm > Th L+V (L)]. Halite dissolution in these inclusions occurs at temperatures of 191°C–305°C, which indicates equivalent fluid salinities of 31–39 wt% NaCl; disappearance of the vapor bubble occurs at 181°C–248°C.

## TEMPERATURES OF FLUID ENTRAPMENT

Pressures of entrapment for the liquid-dominated, low-salinity inclusions in samples from Hole 894G are higher than the equilibrium vapor pressure and, therefore, a temperature correction may be applied to obtain temperatures of fluid entrapment (Roedder, 1984). The difference between homogenization temperatures of inclusions along the liquid-vapor curve and the temperatures of entrapment, is a function of the entrapment pressure and of fluid composition. Temperature corrections were obtained using the equations of Zhang and Frantz (1987) assuming an average fluid composition of 3.2 wt% NaCl equivalent and that hydrostatic pressure conditions apply (10 MPa/km H<sub>2</sub>O). Pressures of entrapment were calculated using the ex-

panded sample recovery depth and an overlying water column of 3460 m. For the inclusions that homogenize at temperatures of ~200°C–370°C, temperatures of entrapment range from 230°C to 416°C at a pressure of 50 MPa and 266°C to 506°C at a 100-MPa entrapment pressure, respectively (Fig. 12).

## FLUID EVOLUTION

### High-salinity Fluid Inclusions

Halite-bearing fluids have been noted for many years in fossil hydrothermal systems associated with land-based ore deposits (e.g., Gustafson and Hunt, 1975; Ahmad and Rose, 1980; Bodnar and Beane, 1980; Reynolds and Beane, 1985); however, only recently have they been recognized in high-temperature submarine environments (Kelley and Delaney, 1987; Vanko, 1988; Kelley and Robinson, 1990; Kelley et al., 1992, 1993; Vanko et al., 1992; Kelley, 1994). The high-salinity inclusions in gabbros recovered from the Hess Deep are the first reported occurrence of brines from a fast-spreading ridge. Formation of halite-bearing fluids in porphyry copper and submarine systems has been attributed to condensation (supercritical phase separation) of brine droplets from a low-salinity vapor of either magmatic or meteoric/seawater origin and direct exsolution of a high salinity fluid from late stage melts (Cline and Bodnar, 1991; Kelley et al., 1992, 1993). Below we evaluate the role of aqueous immiscibility and fluid exsolution in the generation of brines in the gabbros from Site 894.

### Condensation

Compositions of submarine hydrothermal vent fluids from 9°N on the East Pacific Rise (Von Damm, 1990; Von Damm et al., 1992), and from Axial Seamount (Butterfield et al., 1990; Butterfield et al., 1994) and the Endeavour Segment on the Juan de Fuca Ridge (Lilley et al., 1993), indicate that deep-seated, supercritical phase separation most likely plays an important role in determining vent fluid chemistry. Salinity variations of hydrothermal solutions from >70% below to 200% above seawater concentrations, in conjunction with covariant enrichment and depletion of gas phases, respectively, are believed to result from subsurface mixing of modified seawater with gas-enriched vapor phases and gas-depleted brines generated during previous phase separation events. Compelling evidence that aqueous im-

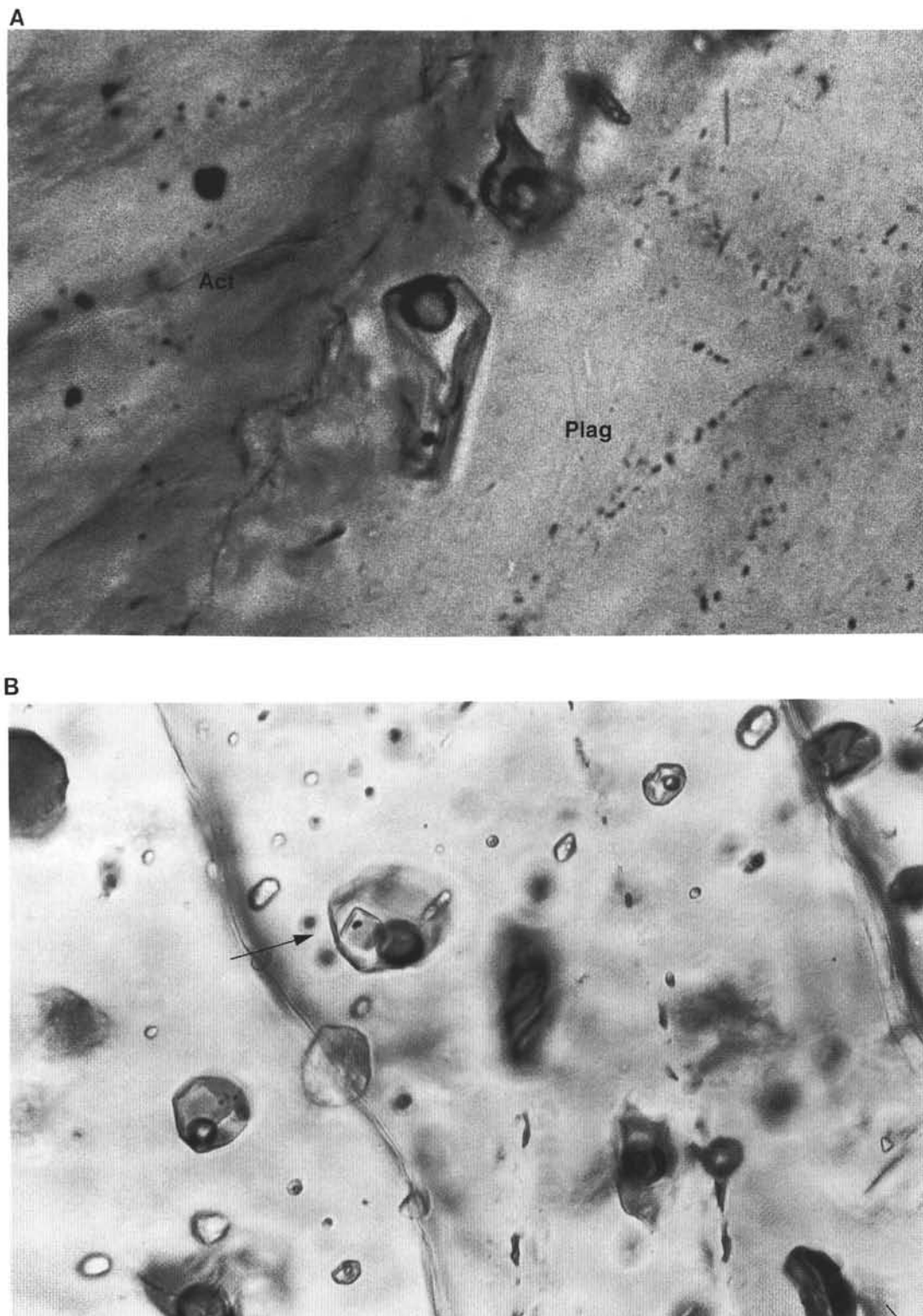


Figure 7. Photomicrographs of fluid inclusion types 1 and 3. **A.** Type 1, plagioclase-hosted (Plag), liquid-dominated secondary inclusion adjacent to actinolite (Act) after clinopyroxene. The largest inclusion is 12  $\mu\text{m}$  in length. **B.** Type 3, liquid-dominated fluid inclusion in plagioclase. The brine-rich inclusions contain a moderate-sized vapor bubble that is rimmed by a high-salinity liquid and a halite daughter mineral (arrow) that hosts a fine-grained opaque mineral. Central inclusion is 22  $\mu\text{m}$  in length.



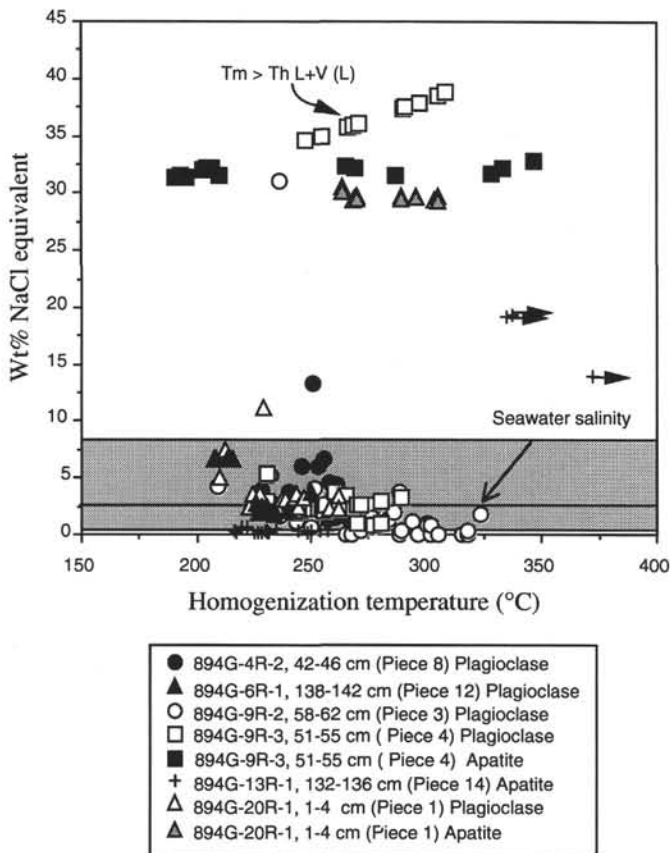


Figure 8. Uncorrected homogenization temperatures and corresponding equivalent fluid salinities for gabbro-hosted inclusions from Hess Deep, Hole 894G. The fluid inclusions exhibit a bimodal salinity distribution. Brine-rich inclusions that form a gentle, positively sloped curve homogenize by halite dissolution [ $T_m > T_h L + V (L)$ ]. Those that lie in the field just to the right of the curve homogenize by disappearance of the vapor phase. Low-salinity fluids that contain equivalent fluid salinities from ~0.1% to 200% of seawater values (3.2 wt% NaCl) exhibit a striking overlap in composition with fluids exiting hydrothermal vents (stippled field). Symbols for fluid inclusion samples used in this study are identified also for the minerals hosting the inclusions. Arrows indicate minimum homogenization temperatures for inclusions in Sample 147-894G-13R-1, 132–136 cm (Piece 14).

miscibility occurs in the seafloor has been provided by the discovery of cogenetic brine and low-salinity, vapor-filled fluid inclusions in metagabbros from MARK (Fig. 9) (Kelley and Delaney, 1987; Kelley et al., 1993) and in quartz-bearing veins in metagabbros from the failed Mathematician Ridge (Vanko, 1988). High-salinity inclusions in metagabbros from the Oceanographer Fracture Zone (Vanko et al., 1992), and the Semail (Nehlig and Juteau, 1988) and Troodos ophiolites (Figs. 9, 11) (Kelley and Robinson, 1990; Kelley et al., 1992) have also been cited as evidence for phase separation. In the following discussion we present two scenarios for immiscibility by applying magmatic and seawater source models.

### Magmatic Fluid Source

In submarine environments, halite-bearing fluids of obvious magmatic origin have been recognized only in gabbroic rocks from the MARK area (Kelley and Delaney, 1987; Kelley et al., 1993), though they are characteristic of high-temperature plutonic environments associated with porphyry copper deposits. The primary inclusions from MARK are oriented parallel to fluorapatite crystal faces and exhibit a continuum between  $\text{CO}_2$ -rich and  $\text{CO}_2$ -poor brines that coexist with

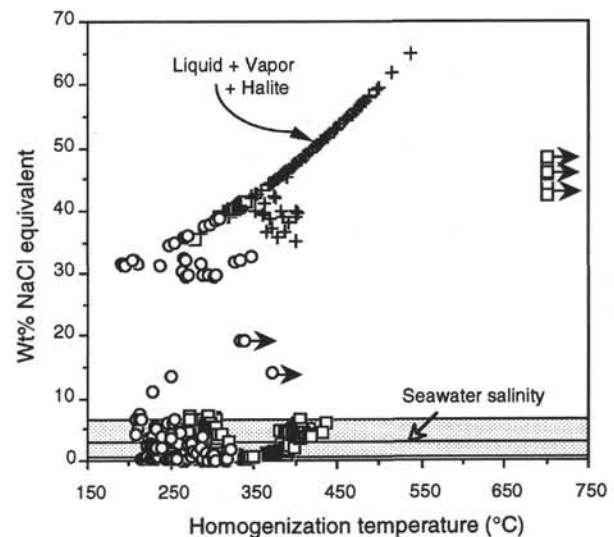


Figure 9. Corresponding homogenization temperatures and equivalent fluid salinities of plutonic-hosted fluid inclusions in submarine environments. The primary? and secondary inclusions in the Hess Deep gabbroic rocks (circles) exhibit a compositional evolution similar to that observed in upper level gabbroic and plagiogranitic rocks from the Troodos ophiolite (crosses) and gabbros and trondhjemitic rocks recovered from the MARK area on the Mid-Atlantic Ridge (squares). Brine-rich inclusions that form the gentle, positively sloped curve (liquid + vapor + halite) may represent brines exsolved directly off of late-stage melts at shallow crustal depths. Fluorapatite-hosted inclusions in gabbros from MARK remain unhomogenized at temperature  $>700^\circ\text{C}$  (arrows). The inclusions contain magmatic  $\text{CO}_2$ - $\text{H}_2\text{O}$ -NaCl-rich brines and vapors that were exsolved under immiscible conditions. Arrows on Hess Deep samples indicate minimum homogenization temperatures for inclusions in Sample 147-894G-13R-1, 132–136 cm (Piece 14) (see text for discussion).

$\text{CO}_2$ - $\text{H}_2\text{O}$ -vapor-dominated inclusions. The primary inclusions, which remain unhomogenized at temperatures  $>700^\circ\text{C}$ , provide unequivocal evidence for a magmatic origin (Fig. 9). They are believed to have formed by immiscibility as residual evolved melts reached water saturation and immiscible  $\text{CO}_2 + \text{H}_2\text{O} + \text{NaCl} \pm \text{Fe}$ -rich brines ( $>50$  wt% NaCl) and cogenetic  $\text{H}_2\text{O}$ - $\text{CO}_2$ -rich vapors (1–2 wt% NaCl) were exsolved at ~1-kb pressure. Spatially related brine- and vapor-rich fluid inclusions are extremely rare in gabbroic rocks recovered from Hole 894G, and thus, several scenarios of formation are possible for the halite-bearing inclusions that homogenize by vapor bubble disappearance (Table 2; Figs. 8, 11). Because most of the inclusions are dominated by aqueous high-salinity fluids and freezing measurements indicate that evidence for  $\text{CO}_2$  is rare, the conditions under which the fluids were entrapped may be predicted using the system NaCl- $\text{H}_2\text{O}$ .

In the Hess Deep gabbros, a magmatic source model for the formation of halite-bearing inclusions that homogenize to the liquid phase suggests that the fluids were exsolved from evolved interstitial melts. In mid-ocean ridge systems, the incompatible nature of  $\text{H}_2\text{O}$  in melts of basaltic composition, coupled with its low concentration, means that  $\text{H}_2\text{O}$  does not become saturated until the late stages of melt fractionation. For example, assuming an initial water content of 0.2 wt%, a basaltic melt (MORB) emplaced 2–3 km beneath a ridge axis will not become saturated with respect to water until ~95% crystallization (Burnham, 1979). Such conditions are probably not achieved until temperatures of  $\sim 700^\circ\text{C}$ – $800^\circ\text{C}$  (Wyllie, 1977; Burnham, 1979). The salinity of the exsolved aqueous phase is determined by the chlorine content of the melt and the partition coefficient between the melt and the volatile phase. Compositions of the immiscible phases are dependent only on the temperature and pressure at

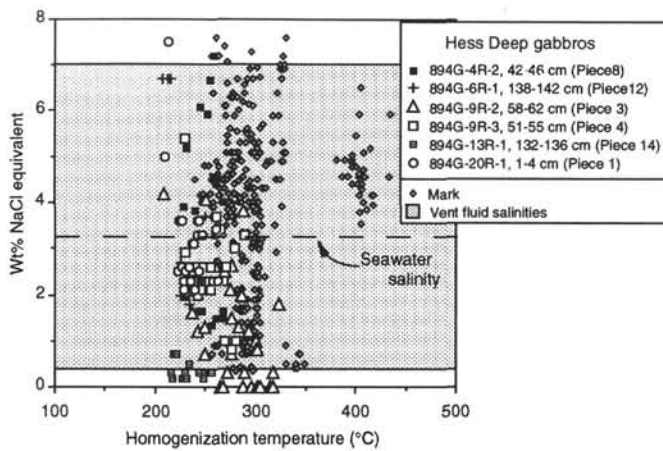


Figure 10. Uncorrected homogenization temperatures and corresponding fluid salinities for low-salinity, gabbro-hosted inclusions from Hess Deep, Hole 894G, and from the MARK area. Homogenization temperatures of fluid inclusions from the Hess Deep are slightly lower than those in gabbroic rocks from the MARK. Secondary inclusions in the Hess Deep gabbros record some of the lowest-salinity fluids reported for deep-seated submarine hydrothermal systems, and are lower than those of fluids exiting active hydrothermal vents on the seafloor (stippled area). Such low salinities at Hess Deep may be achieved only during supercritical phase separation at pressures <50 MPa.

which immiscibility occurs and are independent of the parental fluid salinity (see Kelley et al., 1993, for a more detailed discussion). Depending on the initial bulk composition of these evolved fluids, and the temperature and pressure under which volatile exsolution occurs, fluids may be exsolved from the melt as either immiscible (i.e., vapors and brines) or homogeneous phases.

The temperature-depth-pressure relationships under which immiscibility occurs for the NaCl-H<sub>2</sub>O system are shown in Figure 13 (after Fournier, 1987; and Bodnar, 1994). The critical curve, which connects the critical points for fluids of varying salinities, separates the one-phase, liquid field from the two-phase, liquid + vapor field. In highly permeable zones in which open fractures extend to the seafloor, fluid pressures may be approximated by hydrostatic conditions (curve labeled  $P_h^i$ ). If the rock is molten or falls within the field of ductile deformation, the pressure exerted on the fluid may be more closely approximated by computing the combined load of the overlying masses of seawater and rock. The more gently sloped curve labeled  $P_l^i$  schematically shows the position of the two-phase curve for a 3.2 wt% NaCl salinity fluid under lithostatic conditions, assuming that there is a transition from hydrostatic to lithostatic pressures at 35 MPa (corresponding to an overlying water column of 3500 m) and a rock density of 2.85 g/cm<sup>3</sup>. Because of the nearly 3/1 pressure-depth relationship on the position of the two-phase curve under lithostatic conditions, the field of immiscibility is compressed such that brine and vapor formation is restricted to shallow crustal levels. The intersection of the two-phase curve and the water-saturated solidus bounds the field where brines and vapors will be exsolved from a melt assuming a parental fluid salinity of 3.2 wt% NaCl. If the magmatic fluids initially were higher in salinity or were CO<sub>2</sub>-rich, the position of the two-phase field would extend to higher pressures, and phase separation could occur at deeper crustal levels (Frantz et al., 1992).

A possible scenario for formation of the halite-bearing inclusions that homogenize to the liquid phase may involve exsolution of aqueous fluids into the two-phase field from late-stage interstitial melts (Fig. 13) at temperatures of ~700°C–800°C. If the inclusions represent fluids that were entrapped in primary magmatic phases during mineral growth, this model requires that exsolution occurred at pressures of 120–140 MPa. At temperatures of ~700°C–800°C and at

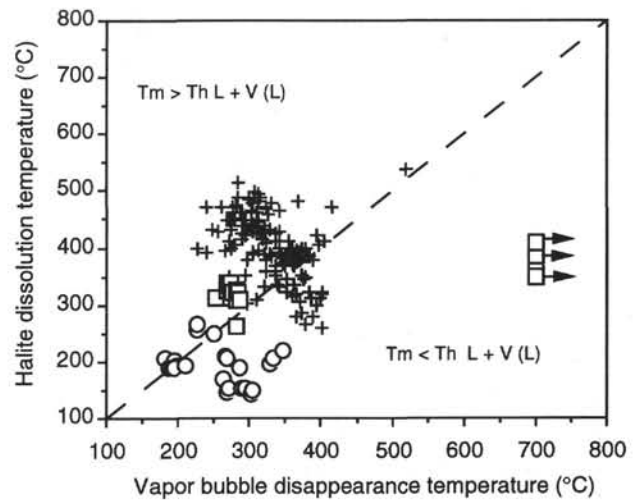


Figure 11. Corresponding vapor bubble disappearance temperatures and halite dissolution temperatures for halite-bearing inclusions in gabbroic rocks from the Hess Deep (circles), upper level gabbroic and plagiogranitic rocks from the Troodos ophiolite, Cyprus (crosses), and gabbroic and rare trondhjemitic rocks from near the MARK area of the Mid-Atlantic Ridge (squares). Inclusions that lie along the dashed line are those in which vapor bubble disappearance and halite dissolution occurs at the same temperature. Inclusions that lie in the field just to the right of the dashed line homogenize by vapor bubble disappearance. Halite dissolution temperatures indicate that these inclusions in the Hess Deep rocks contain equivalent fluid salinities of 29–32 wt% NaCl. Halite-bearing inclusions that fall in the field to the left of the 1:1 line homogenize by halite dissolution and contain equivalent fluid salinities of 31–39 wt% NaCl. Arrows indicate that the MARK inclusions remain unhomogenized at temperatures >700°C.

pressures less than or greater than 120–140 MPa, immiscibility would result in brines with respective salinities less than or greater than the ~30–40 wt% NaCl fluids observed in the Hess Deep gabbro, respectively (Bodnar et al., 1985). These pressures correspond to entrapment depths of ~3 km below the recovery depth of the gabbros from Hole 894G. A pressure correction of several kilobars, however, is necessary to achieve entrapment temperatures of 700°C for 40 wt% fluids that homogenize at temperatures of ~250°C (Bodnar, 1994). Therefore, it is unlikely that the brine-rich inclusions represent direct entrapment of immiscible magmatic fluids. Arrays of brine-rich inclusions in the Hess Deep gabbros that are clearly entrapped along healed microfractures may, however, represent circulating magmatic fluids that underwent significant cooling prior to inclusion entrapment. Segregation and isolation of the brine and vapor phases as a result of differences in density and wetting characteristics may have allowed the vapors to migrate to more shallow crustal levels, resulting in brine accumulation at depth (Goldfarb and Delaney, 1988; Fox, 1990; Kelley et al., 1992).

The phase separation model may also account for the brine-rich inclusions that homogenize by halite dissolution. As discussed by Bodnar (1994), continued cooling of brines that are formed by phase separation may move the fluids out of the two-phase field and into the pressure and temperature region of trapping in which inclusions homogenize by halite dissolution. In the Hess Deep gabbros, such fluids may be represented by inclusions that exhibit vapor bubble disappearance temperatures of 181°C–248°C and halite dissolution at 191°C–305°C (Figs. 8, 11).

Although the formation of brines by condensation is widely regarded as the dominant mechanism for generating the extreme salinity variations observed in submarine plutonic rocks and in some vent fluids (Delaney et al., 1987; Kelley and Delaney, 1987; Vanko, 1988; Bischoff and Rosenbauer, 1988; Von Damm et al., 1992), the exso-

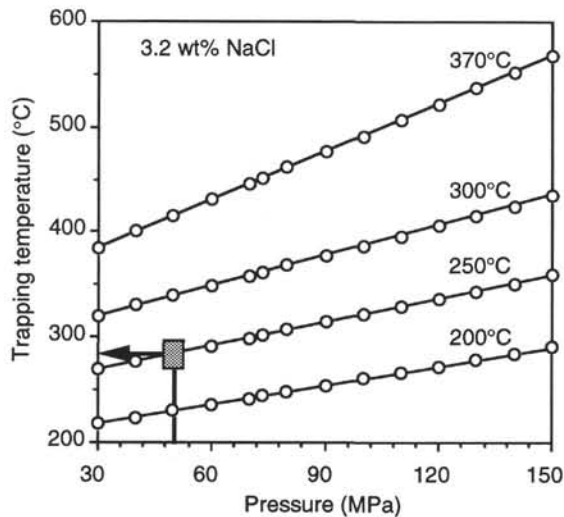


Figure 12. Entrapment pressures and corresponding trapping temperatures for fluid inclusions that contain equivalent fluid salinities of 3.2 wt% NaCl, and homogenize to the liquid phase at temperatures of 200, 250, 300, and 370°C, using the equations of Zhang and Frantz (1987). An entrapment temperature of 270°C is indicated for inclusions that exhibit homogenization temperatures of 250°C and that were trapped under 50-MPa pressure (stippled box).

lution of brines directly off of late stage melts may also play a role in brine generation (Cline and Bodnar, 1991; Kelley et al., 1993). Theoretical modeling of fluid evolution in silicate melts indicates that highly saline fluids may be exsolved directly off of late-stage melts in low-pressure environments (Cline and Bodnar, 1991). It may be that the halite-bearing inclusions that homogenize by halite dissolution represent directly exsolved brines that cooled prior to inclusion entrapment. The inclusions are similar to trondhjemitic-hosted inclusions from the MARK area (Kelley et al., 1993) and to inclusions that occur throughout the plutonic sequence of the Troodos ophiolite, Cyprus (Kelley et al., 1992). In the gabbros from Hole 894G, as well as in the Troodos ophiolite, the observations that brine-rich inclusions occur only in the most compositionally evolved rocks, coupled with the virtual absence of vapor-dominated inclusions are consistent with brine exsolution as a model for brine formation.

### Seawater Source

In an evolving magma-hydrothermal system, as seawater-derived fluids migrate to depth, the fluids must traverse a series of compositionally dependent condensation curves (Fig. 13). Under hydrostatic conditions a fluid of seawater-like salinity (3.2 wt% NaCl) migrating at a crustal depth of 2 km (42 MPa assuming an overlying water column of 2.2 km) and at temperatures of 480°C–500°C would be immiscible and would exist as 30–40 wt% NaCl brines in equilibrium with vapors containing 0.5–1.0 wt% NaCl (Bodnar et al., 1985; Bischoff, 1991). Phase segregation, coupled with cooling and isolation of the brine and vapor phases during migration along the microfracture networks, would preserve the temperature-compositional relationships of the Hess Deep inclusions that homogenize by vapor bubble disappearance. As discussed in the magmatic model, inclusions that exhibit evidence of homogenizing by halite dissolution may represent cooling and subsequent entrapment of the phase-separated brines (Bodnar, 1994).

From the fluid inclusion data alone, it is difficult to constrain a unique origin of the brines in the Hess Deep gabbros. The close association of halite-bearing inclusions with evolved pockets of crystallized melt (these are especially well developed in Section 147-894G-9R-3), coupled with the preliminary data that suggests that some of

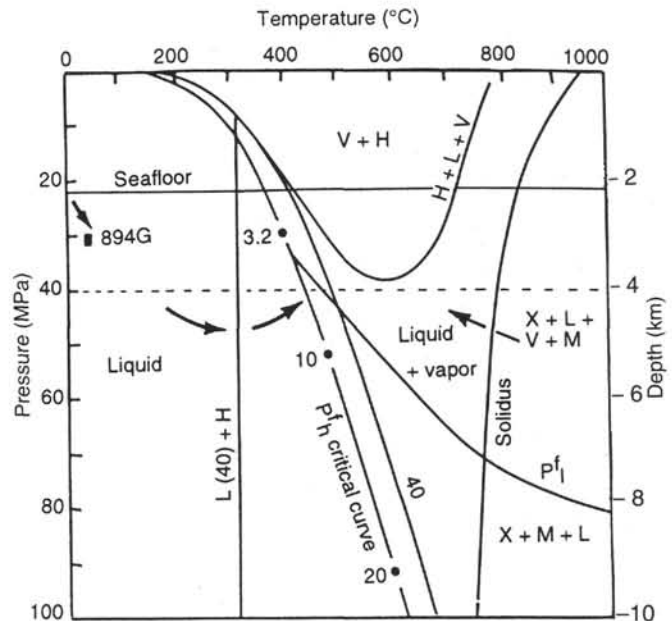


Figure 13. Temperature-depth-pressure relationships in the NaCl-H<sub>2</sub>O system. The critical curve (labeled  $P_h^f$ ) connects the critical points of fluids that contain 3.2, 10, and 20 wt% NaCl salinities and separates the one-phase liquid field from the two-phase liquid + vapor field under hydrostatic conditions. The portion of the curve that corresponds to temperatures and pressures less than the critical point (labeled 3.2 for a fluid of seawater-like salinity) is the boiling curve. The condensation curve corresponds to the portion of the curve that occurs at temperatures and pressures greater than the critical point. The more gently sloped curve labeled  $P_h^f$  schematically shows the position of the two-phase curve for a 3.2 wt% NaCl salinity fluid under lithostatic conditions assuming a seafloor depth of 2200 m, and that the transition from hydrostatic to lithostatic conditions occurs at ~3200 m. The dashed line corresponds to the gabbro/sheeted dike interface. Hole 894G is located at a water depth of 3020 m. Also shown is the two-phase curve for a fluid of 40 wt% NaCl salinity, the halite + liquid + vapor curve (H + L + V), and the vapor + halite field (V + H). The field to the right of the water-saturated solidus (solidus) corresponds to where crystals + vapors + brines (X + L + V + M) would coexist in a melt of evolved composition. Melts saturated with respect to water at pressures ~80 MPa and containing 3.2 wt% NaCl fluids would be exsolved in the one-phase field (X + M + L). For fast-spreading environments, where magma chambers are believed to occur at depths of 2–3 km, aqueous-rich fluids are likely exsolved into the two-phase field as vapors and brines (left pointing arrow). Cooling of 40 wt% brines, formed by condensation, into the pressure and temperature region to the left of the two-phase field, and to the right of the liquids line labeled L (40) + H, would result in trapping of fluids in which inclusions homogenize by halite dissolution. Seawater-derived fluids that migrate to depth must traverse a series of compositionally dependent condensation curves (seawater path). Under hydrostatic conditions a fluid of seawater-like salinity (3.2 wt% NaCl) migrating at a crustal depth of 2 km and at temperatures of 480°C–500°C would be immiscible and would exist as 30–40 wt% NaCl brines in equilibrium with vapors containing 0.5–1.0 wt% NaCl.

the inclusions contain CO<sub>2</sub>, is consistent with a magmatic origin for these fluids. However, additional analyses are needed to further constrain their derivation.

### Low-salinity Fluid Inclusions

Gabbro-hosted, low-salinity inclusions from Site 894 that range from 0.1 to ~20 wt% NaCl, are broadly similar in composition to fluid inclusions in gabbroic rocks recovered from the MARK area (Fig.



10) and in upper level gabbro- and plagiogranite-hosted inclusions from the Troodos ophiolite, Cyprus (Kelley et al., 1992). The low-salinity inclusions in the Hess Deep gabbros typically exhibit equivalent fluid salinities that range from ~0.1% to 200% of seawater values (3.2 wt% NaCl) and exhibit uncorrected homogenization temperatures that cluster at ~250°C (Figs. 8–10). These temperature-compositional relationships require a complex fluid evolution history, which may include the condensation (supercritical phase separation) of magmatic or seawater-derived fluids, variable mixing of hydrothermal seawater with phase-separated brines and vapors, boiling, and rock hydration. In the following discussion, we evaluate these mechanisms and conclude that condensation coupled with segregation was most likely the dominant processes in generating the salinities observed in gabbros from Hole 894G.

Formation of low-salinity vapors and brines by the condensation of seawater has been suggested to be an important process in fossil high-temperature hydrothermal systems in the MARK area (Kelley and Delaney, 1987; Kelley et al., 1993), Oceanographer Transform (Vanko et al., 1992), and at the failed Mathematician Ridge (Vanko, 1988). Using condensation as a model for generation of the ~0.1 wt% equivalent salinity fluids in the Hess Deep gabbros places a maximum depth of fluid entrapment at 5 km. This model is illustrated in Figure 14, an isothermal (P–X) projection for the NaCl–H<sub>2</sub>O system (after Bischoff, 1991). Isoleths (solid lines) of the solubility of NaCl in a vapor phase are shown for 0.1, 1.0, and 5.0 wt% NaCl solutions. Also shown are the halite saturation curve and critical curve under hydrostatic conditions ( $P_h^c$ ). The critical curve separates the one-phase field (Liquid) from the two-phase (Liquid + vapor) field (field bounded by hatch marks). Seawater-like fluids (3.2 wt% NaCl) that enter the two-phase field at temperatures and pressures less than the critical point (Cp) undergo “normal” boiling. At temperatures and pressures greater than the critical point, fluids within the two-phase field exist as droplets of brine within a vapor phase. The condensation model for generation of the ~0.1 wt% equivalent salinity fluids in the Hess Deep gabbros requires that fluid circulation occurred at temperatures >407°C and that the inclusions were trapped at pressures less than ~50 MPa. This pressure estimate is a maximum in that at pressures greater than ~50 MPa, condensation would cause vapors with >0.1 wt% NaCl to separate (Fig. 14).

The pressure estimate places significant constraints on the uplift history of the gabbroic rocks drilled on the intrarift ridge. Assuming that the fluids in the Hess Deep gabbros were circulating under hydrostatic conditions, a pressure of ~50 MPa corresponds to a maximum entrapment depth of 5 km (total water depth and crustal thickness). This entrapment depth, coupled with a total water depth in this area of ~3020 m, constrains the uplift of the gabbroic blocks to ~2 km. This represents a maximum uplift because the calculations assume that fluid migration occurred under hydrostatic pressure conditions. Under lithostatic conditions, the two-phase field is compressed, resulting in a swallowing of where 0.1 wt% NaCl fluids can be generated.

Applying a seawater source and phase separation model in generation of the ~8 wt% NaCl equivalent fluids, and assuming that these fluids represent the brine endmember, places a maximum temperature of entrapment to less than ~425°C (Fournier, 1987). At temperatures greater than this, owing to the strong curvature of the isotherms in the NaCl–H<sub>2</sub>O system, condensation of seawater-like (3.2 wt% NaCl) fluids will generate salinities much higher than the ~8 wt% NaCl equivalent fluids observed in gabbros from the Hess Deep. Because the homogenization temperatures of the low-salinity fluid inclusions cluster at ~250°C, and corresponding entrapment pressures were probably <100 MPa (assuming a water depth of ~3000 m coupled with 2–3 km of overlying crust), the resultant pressure corrections indicate that the vapors most likely cooled at least 50°C–60°C after phase separation.

The compositional and phase relationships of the inclusions reflect a complex history subsequent to phase separation. Preservation of fluids with 0.1 wt% NaCl salinities requires that the vapor and

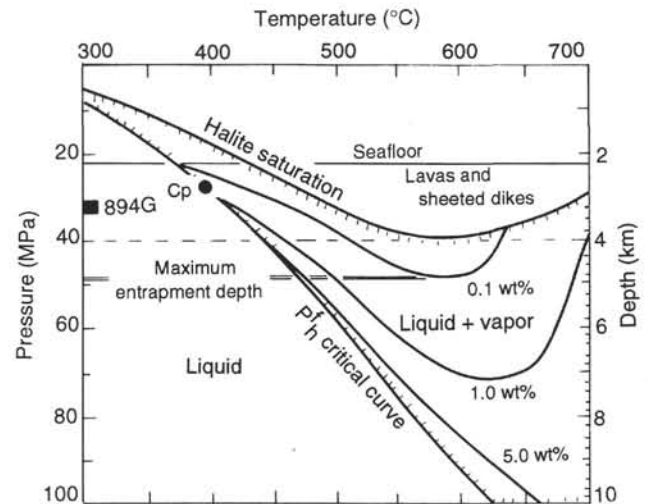


Figure 14. Isothermal (P–X) projection for the NaCl–H<sub>2</sub>O system (after Bischoff, 1991). Isoleths (solid lines) of the solubility of NaCl in a vapor phase are shown for 0.1, 1.0, and 5.0 wt% NaCl solutions. Also shown are the halite saturation curve and critical curve under hydrostatic conditions ( $P_h^c$ ). The critical curve separates the one-phase field (Liquid) from the two-phase (Liquid + vapor) field (field bounded by hatch marks). Seawater-like fluids (3.2 wt% NaCl) that enter the two-phase field at temperatures and pressures less than the critical point (Cp) undergo “normal” boiling. At temperatures and pressures greater than the critical point, fluids within the two-phase field exist as droplets of brine within a vapor phase. The condensation model for generation of the ~0.1 wt% equivalent salinity fluids in the Hess Deep gabbros requires that fluid circulation occurred at temperatures >407°C (the critical point of seawater) and that the inclusions were trapped at pressures less than ~50 MPa. This pressure estimate is a maximum in that at pressures greater than ~50 MPa, condensation would cause vapors with >0.1 wt% NaCl to separate.

brine phases underwent segregation and maintained isolation after phase separation. During the segregation and migration of immiscible fluids, preferential accumulation of the brines occurs at depth, as the lower-density expanded vapor phases migrate upward (Fox, 1990). Such processes are believed to be occurring below active hydrothermal systems at 9°N on the EPR (Von Damm et al., 1992) and on the Endeavor segment of the Juan de Fuca Ridge (Lilley et al., 1993). The temperature and compositional relationships of the low-salinity fluids in the Hess Deep gabbros may reflect similar deep-seated processes.

### Boiling

Progressive boiling and fractional distillation may also generate fluids with salinities depleted and enriched with respect to seawater values. Assuming that the initial fluid salinities were close to seawater values, in order for boiling to be a viable mechanism for the salinity variation observed in the gabbros from Site 894, fluid circulation must have occurred at temperatures less than the critical point of seawater, i.e., less than 407°C and 29.8 MPa pressure (i.e., <2980 m water depth) (Fig. 14). A minimum formation depth of the gabbroic rocks recovered from Hole 894G is ~3023 m (total water depth) and as these rocks were cored from the intrarift ridge, they probably crystallized at somewhat deeper crustal depths. The recovery depth of ~3023 m corresponds to hydrostatic pressures (302 MPa) greater than the critical point of seawater; thus, boiling is unlikely to have played a role in generating the observed fluid salinities. In an evolved hydrothermal system in which the salinity of parental fluids may be enriched with respect to seawater values owing to previous or ongoing distillation or phase-separation events, boiling may play an important

role however. In this case, as residual higher salinity fluids accumulate at depth, the depth at which boiling may occur also increases, reflecting the fact that the higher salinity fluids have correspondingly higher critical point temperatures.

### Hydration

A hydration mechanism for producing the observed variation in salinity requires significant rock hydration in the crust. Under rock-dominated conditions, hydration reactions have the potential of modifying the ionic strength of hydrothermal fluids by consuming or liberating chloride ion. Secondary amphiboles and apatites that contain chlorine may locally act to decrease fluid salinities during hydration processes. Assuming perfect partitioning between chlorine and a hydrous-bearing mineral phase, at least 50% of the gabbros would have to be altered to decrease the salinity of seawater by one-half, or double it if only water is consumed. Thus, it is unlikely that this process played a significant role in generating the observed salinity variation in the Hess Deep gabbros.

In evaluating the models, the extremely low salinities are difficult to account for without invoking condensation. It should be noted that whatever mechanism controls the salinity of these fluids, it is not unique to the Hess Deep area because similar salinity ranges are observed in plutonic-hosted inclusions from MARK (Figs. 9, 10) (Kelley and Delaney, 1987; Kelley et al., 1993), the Troodos ophiolite, Cyprus (Kelley et al., 1992), the Mathematician Ridge (Vanko, 1988), the Oceanographer Transform Zone (Vanko et al., 1992), and the Gorrige Bank (Nehlig, 1991). The striking compositional overlap of these fluids with respect to those measured in active submarine hydrothermal vent systems indicates that the microfracture-bound fluids may represent the fossilized feeder systems for fluids that eventually escape on the seafloor. Similar fluids recently found in epidote-quartz-sulfide mineral-bearing breccias recovered from the northern wall of the Hess Deep Rift (Saccocia and Gillis, 1993) are consistent with this hypothesis.

## DISCUSSION AND CONCLUSIONS

In the gabbroic rocks recovered from Hess Deep, penetrative magmatic fabrics and complex mineral geochemistry, coupled with overprinting secondary mineral phases, compositionally and thermally distinct populations of fluid inclusions, and crosscutting vein networks, indicate that the plutonic sequence experienced multiple magma-hydrothermal pulses as the rocks cooled and were transported away from the zone of crustal accretion. Because of this complicated history, the mineralogical and fluid inclusion results presented in the previous sections are difficult to interpret when considered in an isolated sense, but together provide a working framework with which to begin to constrain the interaction of melts and fluids in fast-spreading environments and their subsequent hydrothermal history.

The mineralogy and textures of the gabbroic samples recovered from Site 894 indicate that the rocks crystallized predominantly from tholeiitic magma (Gillis, Mével, Allan, et al., 1993). However, in isolated pockets, represented by the micropegmatitic gabbros, considerable chemical evolution/modification occurred in the later stages of the crystallization history. In the micropegmatitic patches, textural relationships of the mineral phases, coupled with the trace element geochemistry, suggest that the hydrated mineral assemblage that would normally be considered as a high-temperature hydrothermal metamorphic effect appears to be more related to the buildup and exsolution of aqueous phases in the magmatic stage. In these pods, the chemistry and occurrence of accessory minerals such as apatite, zircon, oxide minerals, and some amphiboles are consistent with crystallization of these phases under relatively high  $fO_2$  and from a hydrous magma. The general restriction of brine-rich inclusions (some of which exhibit evidence for containing  $CO_2$ ) to chlorine-rich apa-

tites and the presence of plagioclase grains within the pegmatitic patches indicate that the earliest magmatic fluids within these zones may have involved exsolution of 30–40 wt% brines.

Melt-mineral relationships within these zones are not straightforward, however, for although these pockets of magma appear fairly evolved in terms of  $TiO_2$ ,  $P_2O_5$ , and incompatible elements, they have low  $SiO_2$  (49.78 wt%) and MgO contents that are average basaltic values (Table 1) and which look most like incompatible enriched basaltic andesites (see Gillis, this volume). In addition, even though the REE patterns of these samples are similar to those of plagiogranitic rocks found in ophiolites, mineralogically they are dissimilar in that they do not contain quartz (Pedersen and Malpas, 1984). Thus, there appears to be a decoupling of the major elements from the trace elements in these samples. The reason for this may be that the major elements and Cr act as compatible elements that are controlled by the framework silicate minerals, and that the incompatible and trace elements are concentrated in a later liquid phase that percolates into this framework at a late stage. Thus, the end product may not represent trapped liquid that at any stage was in equilibrium with the host silicate cumulate, but a liquid that may have been derived by fractionation elsewhere in the system.

An additional puzzling aspect in interpreting the mineralogy and geochemistry of the micropegmatitic patches in terms of an evolved melt is the discrepancy between the silica values and the mineralogical-geochemical results that seem to reflect mineral precipitation under pneumatolytic conditions. Because mid-ocean-ridge melts of basaltic composition typically contain low initial concentrations of dissolved water, given the silica values of ~50 wt%, it is unclear why there is an abundance of magmatic amphibole (see Gillis, this volume). One explanation may be that a significant buildup of volatiles may occur locally as a result of the incorporation and resorption into the melts of partially hydrated diabase inclusions. It is clear that this process is important in the upper level plutonic sequences of ophiolites, and the diabasic inclusions found in Hole 894G indicate that it may be locally important in gabbros from the Hess Deep as well.

The transition from magmatic to hydrothermal seawater-dominated conditions in the plutonic sequence is marked mineralogically by the formation of amphiboles that replace primary mineral phases, and that fill early microfractures and veins. This transition with respect to circulating fluids is marked by fluids that exhibit salinities of <0.1% to 200% of the seawater value and that penetrated into the gabbroic sequence at temperatures of 400°–500° and at maximum pressures of 50 MPa. The enrichment and depletion of fluid salinities, with respect to seawater values, most likely reflect the condensation of seawater-derived fluids that migrated into the plutonic sequence under pressure and temperature conditions corresponding to the two-phase field. Preservation of fluids with 0.1 wt% NaCl salinities within the gabbroic rocks requires that the vapor and brine phases underwent segregation and isolation after phase separation. Interaction of these fluids under greenschist to transition to amphibolite facies conditions resulted in localized pervasive alteration of the plutonic rocks. This alteration is most intense adjacent to vein networks and in cataclastically deformed zones, in which brittle failure facilitated enhanced fluid flow. Sealing of the microfracture and fracture networks with zeolite facies mineral assemblages marks the cessation of fluid circulation in the plutonic sequence. The plutonic sequence may have undergone up to 2 km of uplift attendant with crustal thinning and propagation of the Cocos-Nazca spreading center.

## REFERENCES

- Ahmad, S.N., and Rose, A.W., 1980. Fluid inclusions in porphyry and skarn ore at Santa Rita, New Mexico. *Econ. Geol.*, 75:229–250.
- Bischoff, J.L., 1991. Densities of liquids and vapors in boiling NaCl-H<sub>2</sub>O solutions: a PTVX summary from 300° to 500°C. *Am. J. Sci.*, 291:309–338.
- Bischoff, J.L., and Rosenbauer, R.J., 1988. Liquid-vapor relations in the critical region of the system NaCl-H<sub>2</sub>O from 380°C to 415°C: a refined

- determination of the critical point and two-phase boundary of seawater. *Geochim. Cosmochim. Acta*, 52:2121–2126.
- Bodnar, R.J., 1993. Revised equation and table for determining the freezing point depression of H<sub>2</sub>O-NaCl solutions. *Geochim. Cosmochim. Acta*, 57:683–684.
- , 1994. Synthetic fluid inclusions: XII. The system H<sub>2</sub>O-NaCl. Experimental determination of the halite liquidus and isochores for a 40 wt% NaCl solution. *Geochim. Cosmochim. Acta*, 58:1053–1063.
- Bodnar, R.J., and Beane, R.E., 1980. Temporal and spatial variations in hydrothermal fluid characteristics during vein filling in preore cover overlying deeply-buried porphyry copper-type mineralization at Red Mountain, Arizona. *Econ. Geol.*, 75:876–893.
- Bodnar, R.J., Burnham, C.W., and Sterner, S.M., 1985. Synthetic fluid inclusions in natural quartz. III. Determinations of phase equilibrium properties in the system H<sub>2</sub>O-NaCl to 1000°C and 1500 bars. *Geochim. Cosmochim. Acta*, 49:1861–1873.
- Burnham, C.W., 1979. Magma and hydrothermal fluids. In Barnes, H.L. (Ed.), *Geochemistry of Hydrothermal Ore Deposits*: New York (Wiley), 71–133.
- Butterfield, D.A., Massoth, G.J., McDuff, R.E., Lupton, J.E., and Lilley, M.D., 1990. Geochemistry of hydrothermal fluids from Axial Seamount Hydrothermal Emissions Study vent field, Juan de Fuca Ridge: subseafloor boiling and subsequent fluid-rock interaction. *J. Geophys. Res.*, 95:12895–12921.
- Butterfield, D.A., McDuff, R.E., Mottl, M.J., Lilley, M.D., Lupton, J.E., and Massoth, G.J., 1994. Gradients in the composition of hydrothermal fluids from the Endeavour segment vent field: phase separation and brine loss. *J. Geophys. Res.*, 99:9561–9583.
- Cline, J.S., and Bodnar, R.J., 1991. Can an economic porphyry copper mineralization be generated by a typical calc-alkaline melt? *J. Geophys. Res.*, 96:8113–8126.
- Delaney, J.R., Mogk, D.W., and Mottl, M.J., 1987. Quartz-cemented breccias from the Mid-Atlantic Ridge: samples of a high-salinity hydrothermal upflow zone. *J. Geophys. Res.*, 92:9175–9192.
- Dick, H.J.B., Meyer, P.S., Bloomer, S., Kirby, S., Stakes, D., and Mawer, C., 1991. Lithostratigraphic evolution of an in-situ section of oceanic Layer 3. In Von Herzen, R.P., Robinson, P.T., et al., *Proc. ODP, Sci. Results*, 118: College Station, TX (Ocean Drilling Program), 439–538.
- Fournier, R.O., 1987. Conceptual models of brine evolution in magmatic-hydrothermal systems. *Geol. Surv. Prof. Pap. U.S.*, 1350:1487–1506.
- Fox, C., 1990. Consequences of phase separation on the distribution of hydrothermal fluids at ASHES vent field, Axial Volcano, Juan de Fuca Ridge. *J. Geophys. Res.*, 95:12923–12926.
- Francheteau, J., Armijo, R., Cheminée, J.L., Hekinian, R., Lonsdale, P.F., and Blum, N., 1990. 1 Ma East Pacific Rise oceanic crust and uppermost mantle exposed by rifting in Hess Deep (equatorial Pacific Ocean). *Earth Planet. Sci. Lett.*, 101:281–295.
- Frantz, J.D., Popp, R.K., and Hoering, T.C., 1992. The compositional limits of fluid immiscibility in the system H<sub>2</sub>O-NaCl-CO<sub>2</sub> as determined with the use of synthetic fluid inclusions in conjunction with mass spectrometry. *Chem. Geol.*, 98:237–256.
- Gillis, K., Mével, C., Allan, J., et al., 1993. *Proc. ODP, Init. Repts.*, 147: College Station, TX (Ocean Drilling Program).
- Gillis, K.M., Thompson, G., and Kelley, D.S., 1993. A view of the lower crustal component of hydrothermal systems at the Mid-Atlantic Ridge. *J. Geophys. Res.*, 98:19597–19619.
- Goldfarb, M.S., and Delaney, J.R., 1988. Response of two-phase fluids to fracture configurations within submarine hydrothermal systems. *J. Geophys. Res.*, 93:4585–4594.
- Gustafson, L.B., and Hunt, J.P., 1975. The porphyry copper deposit at El Salvador, Chile. *Econ. Geol.*, 70:857–912.
- Huang, P.Y., and Solomon, S.C., 1988. Centroid depths of mid-ocean ridge earthquakes: dependence on spreading rate. *J. Geophys. Res.*, 93:13445–13477.
- Kelley, D.S., 1994. The influence of spreading rate on fluid evolution in submarine magma-hydrothermal systems. *Eos (Trans. Am. Geophys. Union)*, 75:649.
- Kelley, D.S., and Delaney, J.R., 1987. Two-phase separation and fracturing in mid-ocean ridge gabbros at temperatures greater than 700°C. *Earth Planet. Sci. Lett.*, 83:53–66.
- Kelley, D.S., Gillis, K.M., and Thompson, G., 1993. Fluid evolution in submarine magma-hydrothermal systems at the Mid-Atlantic Ridge. *J. Geophys. Res.*, 98:19579–19596.
- Kelley, D.S., and McDuff, R.E., 1993. Carbon-bearing fluids in the oceanic crust. *Trans. Am. Geophys. Proc.*, 74:654.
- Kelley, D.S., and Robinson, P.T., 1990. Development of a brine-dominated hydrothermal system at temperatures of 400–500°C in the upper level plutonic sequence, Troodos ophiolite, Cyprus. *Geochim. Cosmochim. Acta*, 54:653–661.
- Kelley, D.S., Robinson, P.T., and Malpas, J.G., 1992. Processes of brine generation and circulation in the oceanic crust: fluid inclusion evidence from the Troodos ophiolite, Cyprus. *J. Geophys. Res.*, 97:9307–9322.
- Lilley, M.D., Butterfield, D.E., Olson, E.J., Lupton, J.E., Mackos, S.A., and McDuff, R.E., 1993. Anomalous CH<sub>4</sub> and NH<sub>4</sub> concentrations at an unsedimented mid-ocean ridge hydrothermal system. *Nature*, 364:45–47.
- Nehlig, P., 1991. Salinity of oceanic hydrothermal fluids: a fluid inclusion study. *Earth Planet. Sci. Lett.*, 102:310–325.
- Nehlig, P., and Juteau, T., 1988. Flow porosities, permeabilities and preliminary data on fluid inclusions and fossil thermal gradients in the crustal sequence of the Sumail ophiolite (Oman). *Tectonophysics*, 151:199–221.
- Pedersen, R.B., 1986. The nature and significance of magma chamber margins in ophiolites: examples from the Norwegian Caledonides. *Earth Planet. Sci. Lett.*, 77:100–112.
- Pedersen, R.B., and Malpas, J., 1984. The origin of oceanic plagiogranites from the Karmøy Ophiolite, western Norway. *Contrib. Mineral. Petrol.*, 88:36–52.
- Reynolds, T.J., and Beane, R.E., 1985. Evolution of hydrothermal fluid characteristics at the Santa Rita, New Mexico, porphyry copper deposit. *Econ. Geol.*, 80:1328–1347.
- Riedesel, M., Orcutt, J.A., Macdonald, K.C., and McClain, J.S., 1982. Microearthquakes in the black smoker hydrothermal field, East Pacific Rise at 21°N. *J. Geophys. Res.*, 87:10613–10623.
- Roedder, E., 1984. Fluid inclusions. *Rev. Mineral., Mineral. Soc. Am.*, 12.
- Saccoccia, P., and Gillis, K.M., 1993. Hydrothermal upflow zones in the oceanic crust. *Trans. Am. Geophys. Proc.*, 74:243.
- Sinton, J.M., and Detrick, R.S., 1992. Mid-ocean ridge magma chambers. *J. Geophys. Res.*, 97:197–216.
- Stakes, D., Mével, C., Cannat, M., and Chaput, T., 1991. Metamorphic stratigraphy of Hole 735B. In Von Herzen, R.P., Robinson, P.T., et al., *Proc. ODP, Sci. Results*, 118: College Station, TX (Ocean Drilling Program), 153–180.
- Sterner, M.S., Hall, D.L., and Bodnar, R.J., 1988. Synthetic fluid inclusions. V. Solubility relations in the system NaCl-KCl-H<sub>2</sub>O under vapor-saturated conditions. *Geochim. Cosmochim. Acta*, 52:989–100.
- Toomey, D.R., Solomon, S.C., Purdy, G.M., and Murray, M.H., 1985. Microearthquakes beneath the median valley of the Mid-Atlantic ridge near 23°N: hypocenters and focal mechanisms. *J. Geophys. Res.*, 90:5443–5458.
- Vanko, D.A., 1988. Temperature, pressure, and composition of hydrothermal fluids with their bearing on the magnitude of tectonic uplift at mid-ocean ridges, inferred from fluid inclusions in oceanic layer 3 rocks. *J. Geophys. Res.*, 93:4595–4611.
- Vanko, D.A., Griffith, J.D., and Erickson, C.L., 1992. Calcium-rich brines and other hydrothermal fluids in fluid inclusions from plutonic rocks, Oceanographer Transform, Mid-Atlantic Ridge. *Geochim. Cosmochim. Acta*, 56:35–47.
- Von Damm, K.L., 1990. Seafloor hydrothermal activity: black smoker chemistry and chimneys. *Annu. Rev. Earth Planet. Sci.*, 18:173–204.
- Von Damm, K.L., Colodner, D.C., and Edmonds, H.N., 1992. Hydrothermal fluid chemistry at 9–10°N EPR: big changes and still changing. *Trans. Am. Geophys. Proc.*, 73:524.
- Wyllie, P.J., 1977. Crustal anatexis: an experimental review. *Tectonophysics*, 43:41–71.
- Zhang, Y.-G., and Frantz, J.D., 1987. Determination of the homogenization temperatures and densities of supercritical fluids in the system NaCl-KCl-CaCl<sub>2</sub>-H<sub>2</sub>O using synthetic fluid inclusions. *Chem. Geol.*, 64:335–350.

Date of initial receipt: 2 August 1994

Date of acceptance: 24 February 1995

Ms 147SR-013